THE JOURNAL OF BIOLOGICAL CHEMISTRY VOL. 286, NO. 32, pp. 28466–28475, August 12, 2011

Stability Screening of Arrays of Major Histocompatibility Complexes on Combinatorially Encoded Flow Cytometry Beads*[S]

Received for publication, May 19, 2011, and in revised form, June 14, 2011 Published, JBC Papers in Press, June 16, 2011, DOI 10.1074/jbc.M111.262691

Shi Ling Chew[‡1], Ming Yan Or[‡1], Cynthia Xin Lei Chang[‡§2], Adam J. Gehring[¶], Antonio Bertoletti[¶], and Gijsbert M. Grotenbreg[‡§3]

From the [‡]Department of Microbiology, Department of Biological Sciences, and Immunology Programme, Life Sciences Institute, National University of Singapore, 117456 Singapore, the [§]National University of Singapore Graduate School for Integrative Science and Engineering, Life Sciences Institute, 117456 Singapore, and the [¶]Singapore Institute for Clinical Sciences, Agency for Science Technology and Research, Brenner Centre for Molecular Medicine, 117609 Singapore

The binding and stabilization capacity of potential T cell epitopes to class I MHC molecules form the basis for their immunogenicity and provide fundamental insight into factors that dictate cellular immune responses. We have developed a versatile high throughput cell-free method to measure MHC stability by capturing a variety of MHC products on the surface of streptavidin-coated particles followed by flow cytometry analysis. Arrays of peptide-MHC combinations, generated by exchanging conditional ligand-loaded MHC, could be probed in a single experiment, thus combining the molecular precision of biochemically purified MHCs with high content multiparametric flow cytometry-based assays. Semiquantitative determination of the peptide affinity for the restriction element could also be accomplished through competition experiments using this bead-based assay. Furthermore, the generated peptide-MHC reagents could directly be applied to antigen-specific CD8$^+$ T lymphocyte analysis. The combinatorial labeling of beads allowed straightforward identification by their unique fluorescent signatures and provided a convenient means for extended assay multiplexing.

Class I MHC molecules are crucially tasked with presenting repertoires of peptides at the cell surface for inspection by CD8$^+$ T cells, thereby allowing the immune system to respond to degradation products of proteins that are indicative of exposure to infectious disease or cellular transformation. The rational design of vaccines and immunotherapeutics depends on the accurate identification and characterization of those peptide antigens capable of precipitating a robust immune response. Such efforts are confronted with both an overwhelming diversity of potentially immunogenic peptide sequences and the polymorphism of the MHC system whereby each allelic product has a distinct peptide-binding motif that dictates their interactions. This has led to the development of a myriad of assays to probe either the ability of peptide-MHC (pMHC)[4] molecules to stimulate a specific population of T cells or ascertain the specificity and affinity of the peptide for a particular MHC variant (1–4). Cell-free biophysical methods that employ soluble complexes purified to homogeneity have the advantage of directly measuring the molecular interaction between the peptide and MHC without the confounding effects of simultaneous expression of multiple MHC variants in a cellular context. Limitations on the expeditious and high throughput generation of collections of recombinantly produced pMHC products have largely been resolved with the introduction of conditional ligands for class I human leukocyte antigens (HLAs), (5–7) murine MHC, (5, 8–11), and class II MHC molecules (12) and have been exploited for an ELISA-based MHC stability assay (6, 13). Nevertheless, methods that employ cell lines defective in antigen presentation, where the exogenous addition of peptide can measurably restore MHC surface expression, such as the murine RMA-S (14, 15) or human T2 lines transfected with an MHC of choice (16), remain unceasingly popular. The laborious process of determining to which allelic product the peptide binds is often tolerated because of the simplicity of the assay, the absence of any requirement for specialized or proprietary reagents, and the straightforward read-out by flow cytometry.

Here, we describe a novel method for the site-specific capture of arrays of MHC products on distinctly coded beads, thus creating artificial antigen-presenting surfaces that are compatible with flow cytometry analysis. Each bead set is a collection of beads with a range of distinct fluorescent intensities that can be combinatorially coded with additional dyes, thereby leveraging on the high content multiparametric analysis of flow cytometry. Using the encoded bead sets, the binding properties of MHC molecules can be determined for individual epitopes by measuring the stability of the complex through subunit-specific antibody staining as demonstrated for MHC variants of both human and murine origin. The exact contribution of amino

* This work was supported by Singapore National Research Foundation Research Fellowship NRF2007NRF-RF001-226.
[S] The on-line version of this article (available at http://www.jbc.org) contains supplemental Figs. S1–S5.
[1] Both authors contributed equally to this work.
[2] Recipient of a National University of Singapore Graduate School for Integrative Science and Engineering graduate scholarship.
[3] To whom correspondence should be addressed: Immunology Programme, Centre for Life Sciences #03-05, 28 Medical Dr., Singapore 117456. Tel.: 65-6516-6661; Fax: 65-6778-2684; E-mail: grotenbreg@nus.edu.sg.

[4] The abbreviations used are: pMHC, peptide-MHC; β2m, β2-microglobulin; HLA, human leukocyte antigens; J, 3-amino-3-(2-nitro)phenyl-propanoic acid residue; MES, 4-morpholineethanesulfonic acid; PB, Pacific Blue; PE, phycoerythrin.

acids within a T cell epitope to MHC binding and T cell recognition can be explored as exemplified here by alanine, arginine, and aspartic acid scan analysis. By employing fluorescently labeled peptide ligands, the assay can be also modified to accommodate peptide competition assays through which the affinity of particular ligands for their MHC counter structure can be precisely quantified, further showcasing the versatility of this technology.

EXPERIMENTAL PROCEDURES

Peptides

Synthetic peptides used for epitope screening and the FITC-labeled A*02:01 competitor peptide, FLPSD(K-FITC)FPSV were obtained from GenScript (Piscataway, NJ) with a purity of >70% and >90%, respectively. Conditional ligands that incorporate the photocleavable 3-amino-3-(2-nitro)phenyl-propanoic acid residue (J), SV9-P7* (FAPGNY-J-AL) for H-2K^b and H-2D^b (8), and GILGFVF-J-L for A*02:01 (5) were synthesized in-house by standard Fmoc (*N*-(9-fluorenyl)methoxycarbonyl)-based solid phase peptide synthesis. The identity and purity of the conditional ligands was confirmed by LC/MS analysis. All of the lyophilized powders were diluted to 10 mg ml^{-1} in 20% H_2O, 80% Me_2SO, and 10 mM tris(2-carboxyethyl)phosphine and stored at −80 °C until further use. Peptide concentrations used for determination of IC_{50} values were calculated by assuming quantitative synthetic yield.

Recombinant MHC Molecules

Following established protocols (17), the human β2m and the luminal portions of the MHC heavy chains H-2K^b, H-2D^b, and HLA-A*02:01 with a C-terminal BirA recognition sequence were recombinantly expressed in *Escherichia coli*. Inclusion bodies were purified, and resolubilized proteins were refolding with conditional ligands SV9-P7* (for H-2K^b), SV9-P7* (for H-2D^b), and GILGFVF-J-L (for A*02:01) into soluble MHC complexes, followed by enzymatic biotinylation and size exclusion chromatography (Akta FPLC equipped with a HiPrep 16/60 Sephacryl S200; GE Life Sciences). Assembled monomers were stored at −80 °C and used within 1 month after thawing. By adding streptavidin-PE (Invitrogen) to the monomer with a final molar ratio of 1:4, respectively, class I MHC tetramers were produced. The tetramers were placed on ice and irradiated for 15 min in a UV cross-linker (CL-1000, UVP) equipped with 365-nm UV lamps at ~10-cm distance. After 1 h of incubation on ice, the tetramers were centrifuged (16,000 × *g*) for 10 min and used without further manipulation.

Flow Cytometry

For data acquisition, an LSR-II flow cytometer (Becton Dickinson) was employed configured for 14 individual fluorescent channels as detailed below. For the violet 405-nm laser: Qdot700, 685LP, 710/50; Qdot655, 635LP, 670/30; Qdot605, 595LP, 610/20; Qdot565, 550LP, 575/25; Qdot525, 505LP, 525/50, Pacific Blue (PB), 450/50. For the blue 488-nm laser: PerCP, 635LP, 695/40; FITC, 505LP, 530/30; SSC, 488/10. For the 561-nm laser: PE-Cy7, 735LP, 780/60; PE-Cy5, 635LP, 670/30; PE-TR, 600LP, 610/20; PE-YG, 585/15. For the 635-nm laser: APC-Cy7, 750LP, 780/60; Alexa700, 685LP, 710/50; APC, 660/20. The instrument was operated with FacsDiva software.

Peptide-MHC Binding Assay

ELISA—The MHC stability ELISA was performed essentially as described earlier (6, 13). Peptide exchange was accomplished as described for the bead-based assay. Precoating of a 384-well flat bottom polystyrene microtitre plate (Corning) was accomplished with 50 μl of streptavidin (Invitrogen) at 2 μg ml^{-1} in PBS. Following 2 h of incubation at 37 °C, the wells were washed with 0.05% Tween 20 in PBS (four times 100 μl) wash buffer, treated with 100 μl of blocking buffer (2% BSA in PBS), and incubated 30 min at room temperature. Subsequently, 25 μl of UV-exchanged samples that were 25× diluted with blocking buffer were added in quadruplicate. The samples were incubated for 1 h on ice, washed with blocking buffer (4 × 100 μl), treated for 1 h with 25 μl of HRP-conjugated anti-β2m (1 μg/liter in blocking buffer) on ice, washed with blocking buffer (four times 100 μl), and developed for 10–15 min with 25 μl of ABTS-solution (Invitrogen), and the reactions were stopped by the addition of 12.5 μl of stop buffer (0.01% sodium azide in 0.1 M citric acid). Absorbance was subsequently measured at 415 nm using a spectrophotometer (Spectramax M2; Molecular Devices).

Beads—Recombinant caged pMHC was diluted to 5 μM using filtered PBS, and the exchange peptides were diluted to 500 μM in Me_2SO. In Eppendorf tubes, 12.5 μl of caged pMHC and 12.5 μl of the diluted peptides were mixed with 100 μl of filtered PBS. The tubes were placed on ice and subjected to irradiation for 15 min in a UV cross-linker (CL-1000, UVP) equipped with 365-nm UV amps. The samples were then incubated for 1 h at 37 °C with shaking, after which each sample was centrifuged for 5 min at 16,000 × *g*. The subsequent steps were performed at room temperature. Fluorescent particles kits Yellow (Spherotech SVFA-2552-6K and SVFB-2552-6K), Pink (Spherotech SVFA-2558-6K and SVFB-2558-6K), and Blue (Spherotech SVPAK-5067-5A and SVPAK-5067-5B) that are surface-coated with streptavidin were used to capture the pMHC. Thus, in a 96-well V-bottom plate (Corning), 20 μl of the fluorescent bead population of choice was washed with 200 μl of $NaHCO_3$ buffer (50 mM, pH 8.5) and pelleted by 5 min centrifuging at 800 × *g*. After removal of the supernatant, the beads were incubated with 100 μl of blocking buffer (2% BSA in PBS) for 30 min with shaking. Subsequently, 25 μl of a designated UV-irradiated pMHC sample was added to the well. Following 1 h of incubation with shaking, (*a*) the beads were washed with blocking buffer (3 × 200 μl) and 50 μl of Pacific Blue anti-human β2m (Biolegend 316310) at 0.5 μg ml^{-1} was added, followed by 20 min of shaking incubation, and subsequently, the beads were washed with blocking buffer (3 × 200 μl) and fixed with 1% paraformaldehyde in PBS, mixed, and transferred to FACS tubes for flow cytometry analysis; or alternatively, (*b*) unoccupied streptavidin binding sites were blocked by the addition of 50 μl of biotin (62.5 mM in PBS) followed by 15 min of shaking, after which beads could be mixed, washed, stained, fixed, and analyzed as described above.

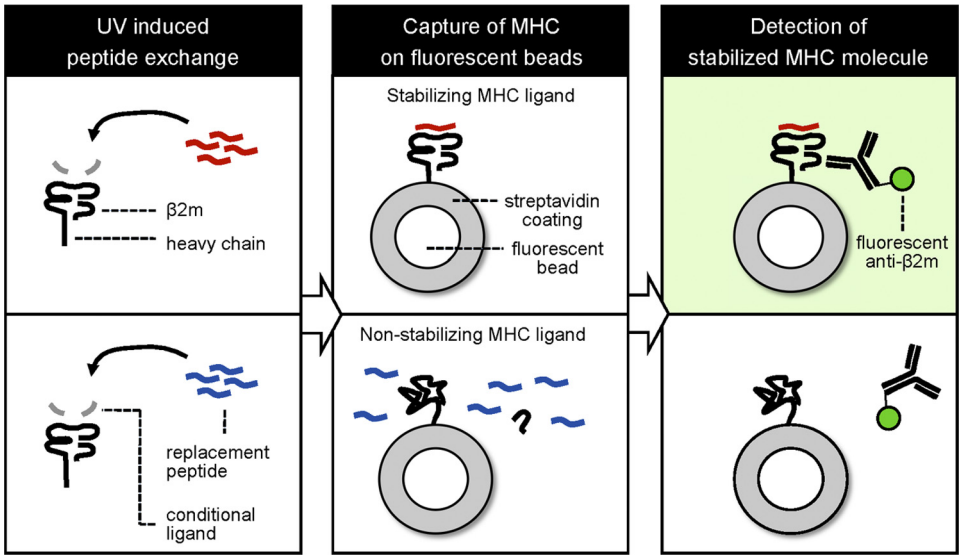

FIGURE 1. **Principle of the MHC stability assay on fluorescent beads.** Recombinantly produced MHC molecules loaded with conditional ligands are exposed to UV light resulting in peptide exchange for a binding ligand (*red*, *top row*) or nonbinding ligand (*blue*, *bottom row*). The emptied MHC molecule is then stabilized and rescued or not stabilized, resulting in its unfolding, respectively. The MHC products are subsequently captured onto streptavidin-coated fluorescent beads, and properly folded complexes can be detected with labeled antibodies that are peptide-specific, MHC conformation-specific, or specific for the noncovalently bound β2m subunit, followed by flow cytometry analysis.

Combinatorial Coding of Fluorescent Beads

The immobilization of secondary colors onto streptavidin-coated fluorescent Yellow (Spherotech SVFA-2552-6K and SVFB-2552-6K) and Pink (Spherotech SVFA-2558-6K and SVFB-2558-6K) particle array kits employed a Live/Dead® fixable near-IR dead cell stain kit (L10119; Invitrogen), whereas Blue beads (SVPAK-5067-10K; Spherotech) were labeled with a Live/Dead® fixable green dead cell stain kit (Invitrogen L23101). The secondary dyes were dissolved in 50 μl of anhydrous Me_2SO according to the manufacturer's instructions. Reconstituted dyes were aliquoted and stable for prolonged periods (>3 months) when stored at −80 °C. In a representative experiment, the Blue bead set was deposited in an 96-well V-bottom plate (Corning) preloaded with 200 μl of $NaHCO_3$ buffer (50 mM, pH 8.5) in three rows of 10 populations (20 μl/independent well) and centrifuged for 5 min at 800 × *g*. After removal of the supernatant, 100 μl of amine-reactive green fluorescent dye solutions that were diluted in $NaHCO_3$ buffer in the ratios 1:80, 1:1280, and no dye (blank) were immediately added to the rows of fluorescent particles, thus furnishing 30 populations of two-dimensionally labeled high (one row), medium (one row), and low (one row) beads, respectively. The mixtures were incubated for 30 min with shaking. Subsequently, unbound secondary color was quenched by washing twice using 200 μl of Tris buffer (50 mM, pH 8), and a further 30 min of shaking incubation with 200 μl of Tris buffer, before pelleting the beads at 800 × *g* for 5 min. These particles with unique fluorescent signature were either directly taken up in 1% paraformaldehyde in PBS, mixed, and transferred to FACS tubes for flow cytometry analysis or used in the beads-based pMHC binding assay.

T Cell Culture and Tetramer Staining

Transduced $CD8^+$ T cell lines specific for HBc_{18-27} were obtained as described earlier and cultured in AIM-V medium (Invitrogen) with 2% pooled human AB serum supplemented with 100 units ml^{-1} of IL-2 for 10 days at 37 °C in a 5% CO_2 atmosphere (18). Short term T cell lines and control T cell lines that were not transduced with the HBc_{18-27}-specific T cell receptor were washed with PBS. Cell viability staining was done using Live/Dead® fixable near-IR stain (Invitrogen) according to the manufacturer's instructions prior to tetramer staining. The cells were washed and stained with 1 μg of PE-conjugated A*0201 tetramers/50 μl of PBS containing 0.1% sodium azide on ice for 20 min. The cells were then stained with Pacific Blue anti-human CD8 (clone RPA-T8; BD Biosciences) for an additional 15 min, washed with PBS, fixed with 1% paraformaldehyde in PBS, and transferred to FACS tubes for flow cytometry analysis.

Data Analysis

Flow cytometry data were analyzed off line with FlowJo Software (Tree Star). In the competition assays, which were determined in triplicate for the various peptides, the percentage inhibition of FITC-labeled parent peptide binding was calculated using the formula: $(1 - (MF_{\text{reference+competitor peptide}} - MF_{\text{background}}) \times (MF_{\text{reference peptide}} - MF_{\text{background}})^{-1}) \times 100\%$. GraphPad Prism software (GraphPad) was used for fitting the data to a four-parameter dose-response curve to derive the fifty percent inhibitory concentrations (IC_{50}).

RESULTS

The Concept of the Bead-based Peptide-MHC Binding Assay—The concept of the MHC stability assay performed on fluorescently labeled beads employs caged MHCs that are loaded with conditional ligands (Fig. 1). After UV irradiation, the peptide fragments are believed to be liberated from the complex (5–8, 12). The uncaged complex can be rescued from degradation when UV-mediated cleavage is performed in the presence of a ligand capable of stabilizing the MHC molecule (Fig. 1, *top row*).

TABLE 1
Sequences of peptides used

	Sequence	Restriction element	Source	Protein	Position
P1	GILGFVFTL	HLA-A*02:01	Influenza A virus	Matrix protein 1	58–66
P2	NLVPMVATV	HLA-A*02:01	Human cytomegalovirus	Lower matrix phosphoprotein pp65	495–504
P3	FLPSDFFPSI	HLA-A*02:01	Hepatitis B virus (Genotype B)	Core protein	18–27
P4	SVLAFRRL	H-2K^b	*Toxoplasma gondii*	Tgd057	59–66
P5	SIYRYYGL	H-2K^b	Synthetic superagonist	Synthetic superagonist	NA
P6	SIINFEKL	H-2K^b	*Gallus gallus*	Ovalbumin	257–264
P7	SAVSNLFYV	H-2D^b	*Chlamydia trachomatis* (Serovar L2)	Polymorphic outer membrane protein	612–620
P8	ASNENMETM	H-2D^b	Influenza A virus (A/Puerto Rico/8/1934(H1N1))	Nucleoprotein	366–374
P9	ASFVNPIYL	H-2D^b	*Chlamydia trachomatis* (Serovar L2)	Cysteine-rich membrane protein A	63–71
P10	FLPSDFFPSV	HLA-A*02:01	Hepatitis B virus (Genotype D)	Core Protein	18–27
P11	AVFDRKSDAK	HLA-A*11:01	Human herpesvirus 4 (strain B95-8)	Epstein-Barr nuclear antigen 4	399–408

On the other hand, peptide ligands that fail to stabilize the MHC will allow the disintegration of the complex followed by the dissociation of the noncovalently bound β2m subunit (Fig. 1, *bottom row*). Thus, probing the beads for the presence of β2m with fluorescently labeled antibodies is a measure of the ability of a ligand to stabilize the MHC. The site-specific immobilization of the MHC to the bead by streptavidin-biotin interaction is a strict requirement, because the indiscriminate conjugation of the complex by alternative chemistries could impede the release of the β2m subunit.

Detection of Various MHC Products on Beads—As proof-of-principle, we employed the odd-numbered set of Pink beads whose increasing intensity of fluorescence could be readily distinguished in both the PE and PE-TR channels (supplemental Fig. S1). This provided a platform of six independent bead populations onto which we could capture and detect simultaneously the various MHC molecules. We exchanged HLA-A*02:01 holding the UV-light sensitive GILGFVFJL (where J denotes the 3-amino-3-(2-nitro)phenyl-propanoic acid (Anp) residue) with ligands P1, P2, and P3 (Table 1) and then loaded each exchange reaction onto an individual bead population. Bead populations presenting distinct pMHC combinations were mixed into a single tube and stained for β2m to monitor class I MHC stability. For controls, the soluble MHC molecules were either not exposed to UV irradiation (−UV), irradiated in the absence of peptide (+UV), or irradiated in the presence of noncanonical epitope P6. The four conditions in which HLA-A*02:01 was predicted to remain stabilized (*i.e.* the canonical epitopes and −UV, corresponding to peaks 1, 3, 7 and 11) show an approximate 7-fold increase in mean fluorescence in the PB channel for β2m (Fig. 2*A*), as compared with the negative controls (*i.e.* populations 5 and 9).

To demonstrate that this assay could be successfully used for a variety of MHC products, we turned our attention to the murine H-2K^b and the H-2D^b gene products bound with the SV9-P7* ligand (8, 9, 11). Conveniently, human β2m readily associates and stabilizes both murine MHCs (19–22), thus affording the possibility of employing the same anti-β2m antibodies for detection as used for HLA molecules. In fact, the xenogenic complex, consisting of human β2m and murine class I MHC heavy chains, has improved stability and peptide binding potential as compared with that of the syngenic complex. The increased stability imparted by human β2m was envisioned to improve the overall peptide binding capacity of the complex, thereby facilitating the detection of weakly binding ligands in the bead-based assay. In the case of H-2K^b, an

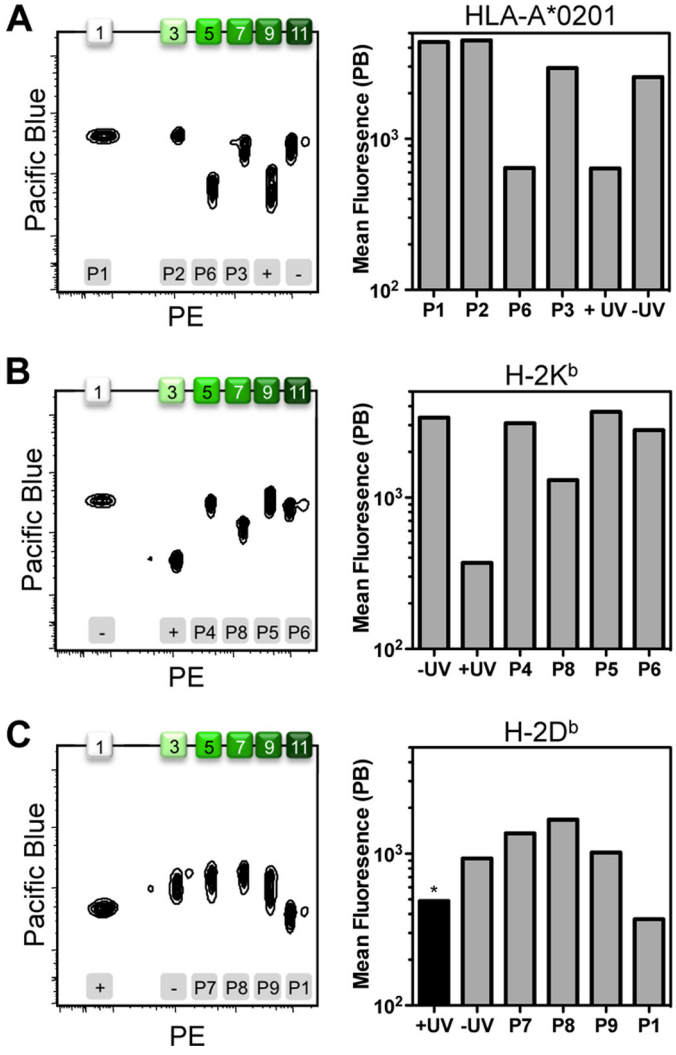

FIGURE 2. **Detection of major histocompatibility complexes on fluorescent beads.** Soluble MHC molecules were ligand-exchanged with peptides P1 (GILGFVFTL), P2 (NLVPMVATV), P3 (FLPSDFFPSI), and P6 (SIINFEKL) in combination with the human HLA-A*02:01 (*A*); peptides P4 (SVLAFRRL), P5 (SIYRYYGL), P6 (SIINFEKL), and P8 (ASNENMETM) in combination with the murine MHC product H-2K^b (*B*); or peptides P1 (GILGFVFTL), P7 (SAVSNLFYV), P8 (ASNENMETM), and P9 (ASFVNPIYL) in combination with the murine MHC molecule H-2D^b (*C*). As controls, the different MHCs were treated with (+) or without (−) UV irradiation in the absence of replacement peptide. The resulting MHC products were captured on streptavidin-coated Pink beads that are increasingly fluorescent in a distinct series of peaks. For the six different conditions tested per MHC, the use of only the odd-numbered bead populations (*i.e.* 1, 3, 5 7, 9, and 11) was sufficient. The beads were probed for intact MHC with anti-β2m conjugated with PB. The *black bar* (*) indicates that the H-2D^b control reaction was incubated at 50 °C to drive complex disintegration to completion. Bead populations are numbered on the top *x* axis, whereas the employed exchange conditions are indicated on the bottom *x* axis.

approximate 10-fold increase in β2m staining was observed for the −UV control as well as with T cell epitopes P4, P5, and P6 that are known to stabilize H-2K^b (Fig. 2*B*; populations 1, 5, 9, and 11) when compared with populations 3 and 7, which were exposed to +UV and P8, respectively. For H-2D^b, the dissociation of β2m was less apparent, with only a 5-fold mean fluorescence difference maximally attainable (Fig. 2*C*). For the +UV control, the complex could only be coaxed to loose stability using low pH (MES, pH 6) and elevated temperatures (50 °C).

Thus, variable amounts of MHC, corresponding to the ability of particular epitopes to rescue UV-induced destabilization of conditional ligand-loaded MHC, could be detected on a single series of fluorescent beads. The assay functioned independently of the bead population chosen for detection (*i.e.* the odd numbered peaks 1–11) because the allocation of conditions ensured that each bead population stained both positive and negative for human β2m at least once over the three experiments combined (Fig. 2). Qualitatively, the bead-based assay generated data consistent with that from the established ELISA format for the range of epitopes, MHCs, and control conditions used (supplemental Fig. S2) (6, 13).

MHC Stabilization on Bead Sets with Distinct Colors—We subsequently investigated whether every currently available set of streptavidin-coated beads of the colors Yellow, Pink and Blue, each with their separate range of fluorescence intensities, could be employed for the bead-based assay. For these collections, there was no particular single flow cytometry channel with the available instrument in which all three bead sets were simultaneously nonfluorescent to use one generically labeled antibody to probe for MHC stability (supplemental Fig. S1). Nevertheless, the Blue and Pink beads proved to combine well with PB-conjugated anti-β2m, whereas PE could be used complementary to the Yellow beads. To limit the number of experimental variables, we focused on a single MHC and explored the exact binding parameters of an established HLA-A*02:01-restricted T cell epitope, the decameric hepatitis B virus core 18–27 peptide (HBc$_{18-27}$, FLPSDFFPSV, P10) by alanine scan (23, 24). This entails sequential alanine point substitutions to the epitope to identify amino acid residues critical for either MHC binding or T cell responsiveness. In a single experiment using Yellow beads, binding of all 10 alanine variants to HLA-A*02:01 could be compared with the parent peptide (Fig. 3*A*). It should be noted that in the Qdot525 channel, where maximal resolution of the independent peaks could be accomplished for this bead set, peaks 2 and 3 were insufficiently separated, leaving 11 instead of 12 distinct populations.

We further demonstrated that this type of systematic but conservative amino acid scan can be extended to the larger and positively charged arginine (Fig. 3*B*) on Pink beads or the negatively charged aspartic acid (Fig. 3*C*) on Blue beads, thereby increasing the rigor of the analysis of the contribution of specific residues to MHC binding. From these experiments, it follows that four positions (Phe^{18}, Leu^{19}, Phe^{24}, and Val^{27}) of the HBc$_{18-27}$ epitope were significantly affected by the replacements, with Leu^{19} being most resistant to amino acid substitution regardless of the nature of the side chain. The C-terminal anchor position Val^{27} was averse to the introduction of charged residues, whereas the N-terminal anchor Phe^{18} and central Phe^{24} did not permit the introduction of an Asp or Arg residue, respectively, without negative consequences for peptide binding to HLA-A*02:01, as was expected (25). These data for the multiple amino acid-substituted variants of the P10 epitope generated with the bead-based assay again compared well with the data obtained from established ELISA protocols (supplemental Fig. S3) (6, 13).

Combinatorial Coding of Fluorescent Beads—The streptavidin-coated beads contain internalized fluorescent dyes with narrowly distributed intensity detectable in a select number of channels depending on their individual excitation and emission characteristics, which we refer to as the beads' primary color (supplemental Fig. S1). It occurred to us that the protein coating on the beads surface could in principle be conjugated with additional chromophores, thereby increasing the high throughput capacity of our bead-based multiplexing approach for measuring MHC stability in similar fashion as previously reported for cell-based fluorescent barcoding (26) and the combinatorial coding of fluorescent MHC multimers (27, 28). For the attachment of the secondary color, we used amine-reactive viability dyes that are commonly used for the discrimination of live cells from those that have lost membrane integrity. These fixable dyes are available in a variety of excitation and emission wavelengths, thus providing flexibility and optimal compatibility with the primary colors of the bead sets. We first tested the feasibility of the two-dimensional color coding of beads by pairing the Yellow and Pink beads with the near-IR fluorescent reactive dye (excited by the 635-nm laser) and the Blue beads with the green fluorescent reactive dye (excited by the 488-nm laser) (supplemental Fig. S4). Optimization of the immobilization reaction allowed us to effectively label and resolve up to three populations: Low, Medium, and High, with the low population being the sample that was not exposed to any amine-reactive reagent. Consequently, with this two-dimensional coding scheme, we could generate 33, 36, and 30 populations, each with a unique fluorescent signature, for the Yellow, Pink, and Blue bead collections, respectively. The secondary color did not appear to affect the fluorescence of the primary color of the beads, and when stored at 4 °C under the exclusion of light it remained stable for several weeks (supplemental Fig. S5). This allows the separate preparation and prolonged storage of bead arrays prior to analyte exposure without detrimental effect to their signature fluorescence.

However, are these arrays of combinatorially labeled beads still capable of capturing soluble MHC molecules, and can they be used subsequently for the assessment of its stability? We explored this by exchanging the peptide of the caged A*02:01 complex either with the A*02:01 epitope P1 or with the A*11:01 epitope P11 (Table 1), where the latter should not have appreciable affinity for this particular restriction element. Both biotinylated MHC molecules were then allowed to associate in alternating fashion with the array of Blue streptavidin-coated beads consisting of all 10 primary color bead sets decorated with the green fluorescent secondary color in the three attainable intensities. All bead populations were subsequently mixed into a single tube, washed, labeled with PB-conjugated anti-β2m and acquired. In accordance with previously established methods (26), the deconvolution of the data can be accom-

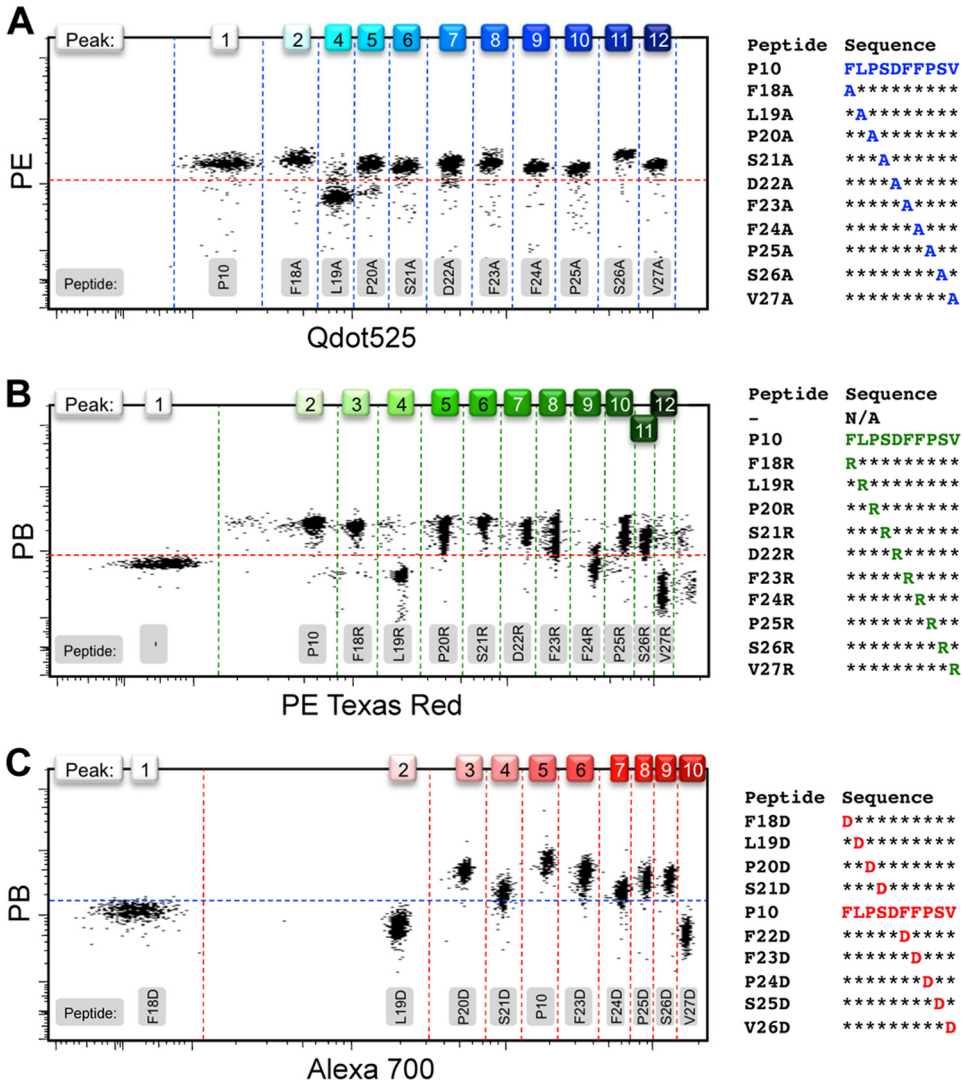

FIGURE 3. **Alanine, arginine, and aspartic acid scans on multiple colored beads.** Individual bead populations were loaded with HLA-A*02:01 molecules that were ligand-exchanged with peptide derivatives of the parent peptide FLPSDFFPSV (P10) in the form of an alanine scan for the Yellow set, where fluorescent peak 3 was omitted because it overlapped with peak 2 too much for them to be clearly distinguishable (*A*), an arginine scan for the Pink set (*B*), and an aspartic acid scan for the Blue set (*C*). MHC stabilization was probed with anti-β2m conjugated with either PB or PE. The choice of color schemes of the bead intensity was deliberately based not on physical appearance of the beads but on the fluorescent emission properties. *Dotted lines* were drawn in arbitrarily after analysis to serve as visual aids and do not represent specific gates.

plished either in forward or reverse fashion depending on whether one focuses first on the original coding strategy of the beads and then the desired phenotypic effect, or vice versa. Starting with the selection of monodisperse beads based on their scatter properties alone, the central plot, the reverse deconvolution (Fig. 4*A*) specifically gates on the PB^+ (*blue*) and PB^- (*black*) populations, corresponding to the presence or absence of intact MHC molecules, respectively. Subsequently, it becomes possible to extricate which coded bead population captured stabilized MHC, correlating with the ability of the replacement epitopes P1 and P11 to stabilize the vacated MHC molecule after uncaging of the complex. Combining both the PB^+ and PB^- data, the *bottom left plot* reveals a checkered ensemble of all 30 populations that are well resolved and appropriately color-coded. Alternatively, the data can be scrutinized by forward deconvolution (Fig. 4*B*), where the beads are gated according to their secondary color first. These three series, low, medium, and high, of 10 bead populations of the same primary color are then assessed independently for the presence of intact MHC, revealing again the alternating patterns of PB^+ and PB^- bead populations, as expected. This type of analysis can be practical when comparing peptide binding properties within a series of different epitopes as, for example, with an alanine scan (Fig. 3).

Competition-based MHC Binding Assay—Apart from the combinatorial labeling of the bead core and surface with a primary and secondary color, respectively, a chromophoric moiety can also be attached to a strategically chosen side chain of a peptide ligand such that the anchor residues and therefore the binding characteristics to the MHC are not adversely affected. When this reporter epitope binds to the uncaged MHC, the fluorescence increases proportionally with the amount of MHC stabilized on the bead surface. The introduction of a second peptide that specifically competes with the fluorescent probe for binding will in turn curtail this. The concentration of competitor peptide at which half-maximal fluorescence is obtained

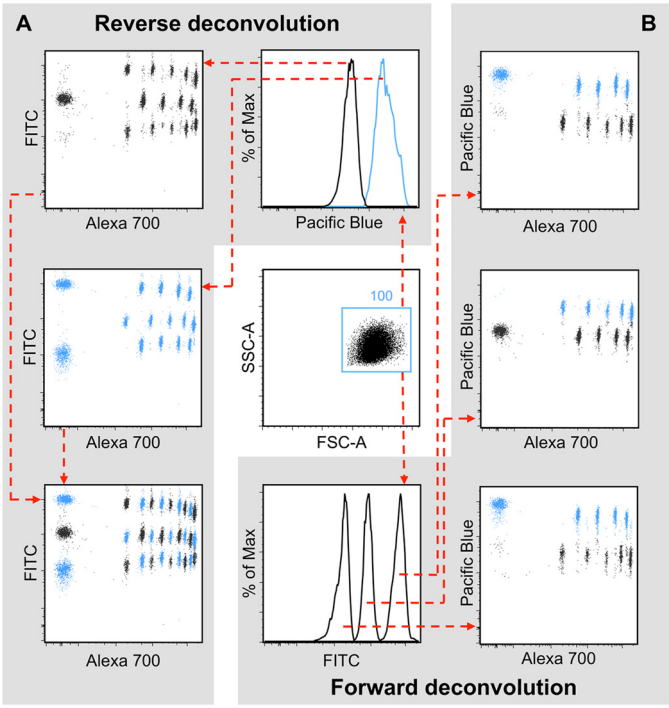

FIGURE 4. **Combinatorial coding of fluorescent beads.** All 10 separate populations of the primary color of Blue beads were coded in three different intensities with fixable green Live/Dead stain as a secondary color to provide 30 individually coded bead populations using protocols developed by Krutzik and Nolan (26). These populations were alternately loaded with HLA-A*02:01 molecules that were ligand-exchanged with either the HLA-A*02:01 epitope P1 or the HLA-A*11:01 epitope P11, which is not expected to bind HLA-A*02:01 and therefore serves as negative control. *A*, reverse deconvolution of the data from single beads (*center dot plot*) starts from gating on either the stabilized (PB^+, *blue histogram*) or the destabilized (PB^-, *black histogram*) MHC molecules. It follows from the coding by the primary color (*x* axis) and secondary color (*y* axis) which beads had stabilized MHC molecules present (*left column dot plots*). *B*, forward deconvolution of single beads (*center dot plot*) is accomplished by gating on one of three different intensities (FITC low, medium, or high histogram) of secondary color labeled beads. This selects 10 separate populations (from the grand total of 30) from where it can be deduced (*right column dot plots*) which beads captured stabilized MHC molecules (PB^+, *blue*) or not (PB^-, *black*).

(IC_{50}) then provides a semiquantitative read-out of the peptide affinity for any particular HLA under investigation (Fig. 5*A*). In a cellular context, this type of peptide binding competition assay has been successfully utilized for a variety of HLA products (29, 30). Accordingly, we based our fluorescent probe on P10 (Table 1), with the exception that a central phenylalanine (Phe^{23}) was replaced with a FITC-conjugated lysine instead of the originally reported iodoacetamido-coupling of FITC to a cysteine side chain for installation of the chromophore (29). The modification of the sixth residue in this peptide does not affect binding to A*02:01 as was demonstrated by the Ala, Arg, and Asp scans (Fig. 3). Our peptide competition experiment on flow cytometry beads showed that at the optimal concentration of probe (~6 μM), a 7–8-fold mean fluorescence increase over background could be obtained. Serial dilution of the competitive ligand markedly restored the FITC signal on the fluorescent beads (Fig. 5*B*). Plotting of the percentage of inhibition against the peptide concentration generated clear sigmoidal inhibition curves for the individual competitive peptides (Fig. 5*C*). Based on the IC_{50} values for HLA-A*02:01 for the HCMV-derived epitope P2 (83 μM) and the hepatitis B virus-derived P10 (23 μM), it is evident that P10 has a higher affinity for the complex than P2, whereas the affinity of the HLA-A*11:01-restricted epitope P11 (>800 μM) for the A*02:01 molecule was negligible. Although side-by-side comparisons have, to our knowledge, not yet been published, and the absolute IC_{50} values are not interchangeable between different peptide-binding assay formats, the affinity ranking of these screened peptides (*i.e.* P2, P10, and P11) corresponds well with data listed publicly at the Immune Epitope Database and Analysis Resource.

Recombinant Peptide-MHC Arrays Allow Direct T Cell Staining—Finally, an important advantage of generating arrays of recombinant peptide-MHC molecules using conditional ligands is that after on-bead assessment of the peptide binding properties, the products can also be multimerized around chromophore-conjugated streptavidin. These soluble complexes can be used directly to stain T cell populations of corresponding

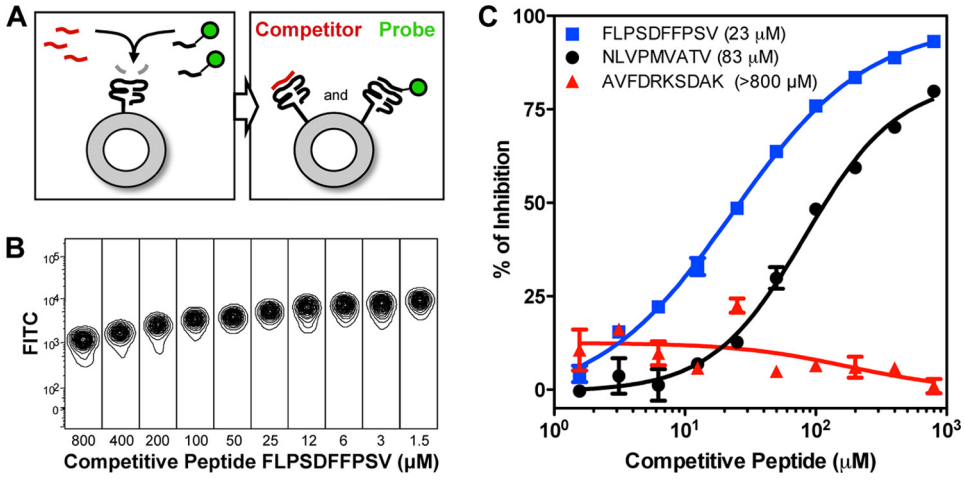

FIGURE 5. **Peptide competition assay.** *A*, the principle of the assay entails peptide competition for the empty peptide-binding site of the MHC molecule after UV cleavage of the conditional ligand. A number of MHC molecules on the bead acquire the probe, whereas other MHC molecules are occupied by the competitor peptide. The final fluorescent signal intensity depends on the concentration of both probe and competitive peptide. *B*, an increase in FITC fluorescence is observed when the probe FLPSD(Lys-FITC)FPSV competes with the serially diluted competitor peptide P10 for binding HLA-A*02:01 molecules captured on Blue beads. *C*, plotting the concentration of competitive peptide as a function of the percentage of inhibition allows the determination of IC_{50} values, as demonstrated for P2 (NLVPMVATV, 83 μM), P10 (FLPSDFFPSV, 23 μM), and P11 (AVFDRKSDAK, >800 μM).

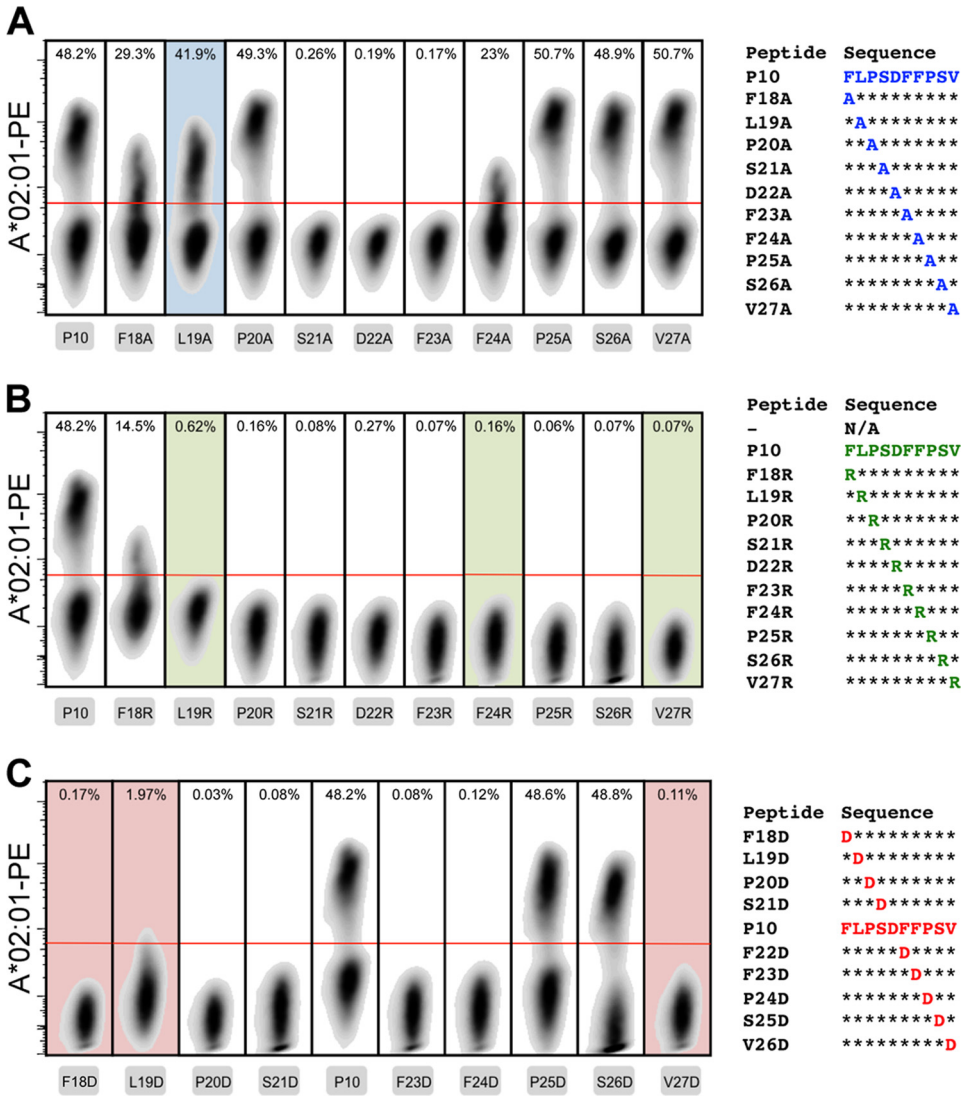

FIGURE 6. **MHC tetramer staining of transduced T cells.** Lymphocytes with an hepatitis B virus core 18–27-specific T cell receptor were obtained through transduction and specifically expanded in culture. PE-conjugated HLA-A*02:01 tetramers that were peptide-exchanged with the alanine (*A*), arginine (*B*), and aspartic acid (*C*) derivatives of parent peptide P10 were evaluated for their capability to stain the lymphocytes specifically gating first on the monodisperse (forward and side scatter), viable (near-IR, Live/Dead negative), and $CD8^+$ (anti-CD8 Pacific Blue-positive) cells. The *red lines* represent the gating for tetramer-positive cells. Plots with shaded backgrounds indicate that after uncaging of the MHC, the peptide was found (by bead-based MHC stability assay and ELISA) to be unable to rescue degradation of the complex.

specificity, enabling the investigation of the role of individual amino acid residues in antigen recognition. We demonstrated this feature by making MHC tetramers of the Ala, Arg, and Asp scan derivatives of the HLA-A*02:01 restricted HBc_{18-27} peptide and evaluated their capability to stain hepatitis B virus-specific lymphocytes that have been transduced with a T cell receptor specific for the immunodominant epitope (Fig. 6) (18). Predictably, the inability of the majority of the peptides that cannot stabilize this restriction element after its uncaging prevents their incorporation in reagents that stain T cells. The destabilizing Ala substitution of the Leu^{19} residue, however, did provide a positively staining reagent. Presumably, the peptide derivative transiently stabilizes the complex when exposed to the T cell staining conditions, without interfering with the peptide-MHC composite surface presented to the T cell receptor. The central residues Ser^{21}, Asp^{22}, and Phe^{23} were found to be critical for recognition because their replacement in all cases abrogated MHC tetramer binding. Indeed, the introduction of the positively charged arginine was overall highly deleterious to antigen recognition, where only the Phe^{18} substitution could be accommodated. The introduction of negative charge posed less stringent constraints for binding to the lymphocytes that received the T cell receptor through gene transfer, because Asp substitution on the Pro^{25} and Ser^{26} positions was without consequence.

DISCUSSION

The accurate definition of peptide affinity and associated class I MHC stability remains vitally important to our understanding of what engenders a productive $CD8^+$ T lymphocyte response and the factors that are its basis. Even though predictive algorithms of peptide binding are constantly being developed and fine-tuned, these bioinformatic tools will continue to rely on experimentally verified data (1–4). The method out-

lined here leverages on the multicolor capabilities of modern flow cytometry for comprehensive analysis of the binding characteristics of arrays of peptides to defined MHC products in a single experimental setting and encompasses a number of distinct advantages. This cell-free system, where beads are homogenously coated to form artificial antigen presenting surfaces, enables the direct and semiquantitative assessment of ligand specificity and affinity for a particular MHC molecule. Assays employing mammalian cells present the challenge that multiple MHC products, as well as additional surface markers, are simultaneously expressed. This can be profoundly affected by culture conditions that confound the interpretation of results. Conditional ligands also significantly speed up the assay, compared with cellular assays (29, 30), and the bead-based stability assay is operated without the need for any radioisotope-labeled peptide or protein. Furthermore, the combinatorial coding of beads employs readily available beads and fixable secondary colors, making the technology operate similarly to suspension arrays such as the BD™ cytometric bead assay, Luminex™, or Bioplex™ assays without the need for proprietary equipment or reagents.

Nonetheless, there are a number of technical aspects that need careful consideration when embarking on MHC stability analysis with this bead-based method. The fluorescent signal of the primary color of the beads is not as narrow as one would anticipate and can be found in the majority of detection channels (supplemental Fig. S1). This either precludes the use of those particular channels or requires rigorous fluorescence compensation and affects the choice of additional chromophores that can be used in a single experiment. For example, we opted to use different antibodies for the various bead collections instead of a single-label anti-β2m antibody. The homogenous conjugation of the secondary color is also crucial for proper resolution of the samples to prevent contamination from neighboring populations and allow accurate deconvolution of the data. Uniform handling of the beads is essential during steps involving individual treatment, so that all populations are present in approximately the same amount during analysis.

Furthermore, conditional ligands are individually designed and validated for discrete MHC products. Striking a balance between the rapid release of the peptide fragments after UV irradiation while maximizing complex stability for high refolding yields and maintenance of structural integrity under normal handling conditions of the protein complex is important (7). For example, the SV9-P7* ligand is cleaved effectively by standard UV irradiation, and peptide exchange can be readily achieved (8). Nevertheless, the H-2D^b complex, be it free of peptide fragments or associated with remnants of the conditional ligand, remained intact for extended periods under these peptide exchange conditions (Fig. 1). This is consistent with published literature, because the human β2m:H-2D^b chimeric complex contains more hydrogen bonds between the heavy and light chain and is more stable than its exclusively murine counterpart (22). An x-ray crystal structure has also shown that the H-2D^b complex was unexpectedly stabilized by a small pentapeptide fragment, indicating that full occupancy of the peptide-binding groove is a less stringent requirement for stability of this complex (31). Fortunately, variables such as incubation time, temperature, and buffer conditions can provide additional control over the assay, although experience with other HLA variants suggests that by and large the standard peptide exchange conditions sufficiently destabilize MHC molecules (data not show) making the stability of the H-2D^b complex a notable exception. Finally, the peptide exchange reaction was also attempted with bead-conjugated MHC (data not show), but this was met with limited success presumably because homogeneous irradiation of the bead surface would minimally require constant agitation of the beads during UV cleavage of the conditional ligand. The use of chemically cleavable conditional ligands, such as the periodate-triggered diol-containing peptides (32) can be expected to perform better, but this line of inquiry was considered outside the scope of the present study.

This proof of concept, however, shows promise for extension in several ways. More uniquely coded bead populations could be generated through higher levels of multiplexing than the two-dimensional coding. By employing more distinct fluorophores to decorate the streptavidin-coated particles, three-dimensional and higher-dimensional coding schemes can be envisioned. Separation on differences in size and granularity also makes it possible to distinguish bead mixtures during data acquisition and analysis based on the forward and side scatter properties. Moreover, the combinatorial coding of beads without detriment to the streptavidin functionality provides the possibility for site-specifically capturing and visualizing other analytes, thus providing an affordable and easily accessible platform technology for the multiparameter analysis of biologically relevant molecules that can be applied in various diagnostic settings.

Acknowledgments—We thank Anthony Tanoto Tan for technical assistance and Dr. Sock Yue Thong for critical reading of the manuscript.

REFERENCES

1. Provenzano, M., Panelli, M. C., Mocellin, S., Bracci, L., Sais, G., Stroncek, D. F., Spagnoli, G. C., and Marincola, F. M. (2006) *Trends Mol. Med.* **12,** 465–472
2. Klug, F., Miller, M., Schmidt, H., and Stevanović, S. (2009) *Curr. Pharm. Des.* **15,** 3221–3236
3. Li Pira, G., Ivaldi, F., Moretti, P., and Manca, F. (2010) *J. Biomed. Biotechnol.* **2010,** 325720
4. Chang, C. X., Dai, L., Tan, Z. W., Choo, J. A., Bertoletti, A., and Grotenbreg, G. M. (2011) *Front. Biosci.* **17,** 3014–3035
5. Toebes, M., Coccoris, M., Bins, A., Rodenko, B., Gomez, R., Nieuwkoop, N. J., van de Kasteele, W., Rimmelzwaan, G. F., Haanen, J. B., Ovaa, H., and Schumacher, T. N. (2006) *Nat. Med.* **12,** 246–251
6. Rodenko, B., Toebes, M., Hadrup, S. R., van Esch, W. J., Molenaar, A. M., Schumacher, T. N., and Ovaa, H. (2006) *Nat. Protoc.* **1,** 1120–1132
7. Bakker, A. H., Hoppes, R., Linnemann, C., Toebes, M., Rodenko, B., Berkers, C. R., Hadrup, S. R., van Esch, W. J., Heemskerk, M. H., Ovaa, H., and Schumacher, T. N. (2008) *Proc. Natl. Acad. Sci. U.S.A.* **105,** 3825–3830
8. Grotenbreg, G. M., Roan, N. R., Guillen, E., Meijers, R., Wang, J. H., Bell, G. W., Starnbach, M. N., and Ploegh, H. L. (2008) *Proc. Natl. Acad. Sci. U.S.A.* **105,** 3831–3836
9. Gredmark-Russ, S., Cheung, E. J., Isaacson, M. K., Ploegh, H. L., and Grotenbreg, G. M. (2008) *J. Virol.* **82,** 12205–12212
10. Frickel, E. M., Sahoo, N., Hopp, J., Gubbels, M. J., Craver, M. P., Knoll, L. J., Ploegh, H. L., and Grotenbreg, G. M. (2008) *J Infect Dis.* **198,** 1625–1633

11. Wilson, D. C., Grotenbreg, G. M., Liu, K., Zhao, Y., Frickel, E. M., Gubbels, M. J., Ploegh, H. L., and Yap, G. S. (2010) *PLoS Pathog.* **6,** e1000815
12. Grotenbreg, G. M., Nicholson, M. J., Fowler, K. D., Wilbuer, K., Octavio, L., Yang, M., Chakraborty, A. K., Ploegh, H. L., and Wucherpfennig, K. W. (2007) *J. Biol. Chem.* **282,** 21425–21436
13. Hadrup, S. R., Toebes, M., Rodenko, B., Bakker, A. H., Egan, D. A., Ovaa, H., and Schumacher, T. N. (2009) *Methods Mol. Biol.* **524,** 383–405
14. Townsend, A., Ohlén, C., Bastin, J., Ljunggren, H. G., Foster, L., and Kärre, K. (1989) *Nature* **340,** 443–448
15. Ljunggren, H. G., Stam, N. J., Ohlén, C., Neefjes, J. J., Höglund, P., Heemels, M. T., Bastin, J., Schumacher, T. N., Townsend, A., and Kärre, K. (1990) *Nature* **346,** 476–480
16. Hosken, N. A., and Bevan, M. J. (1990) *Science* **248,** 367–370
17. Garboczi, D. N., Hung, D. T., and Wiley, D. C. (1992) *Proc. Natl. Acad. Sci. U.S.A.* **89,** 3429–3433
18. Gehring, A. J., Xue, S. A., Ho, Z. Z., Teoh, D., Ruedl, C., Chia, A., Koh, S., Lim, S. G., Maini, M. K., Stauss, H., and Bertoletti, A. (2011) *J. Hepatol.* **55,** 103–110
19. Parker, K. C., DiBrino, M., Hull, L., and Coligan, J. E. (1992) *J. Immunol.* **149,** 1896–1904
20. Pedersen, L. O., Stryhn, A., Holter, T. L., Etzerodt, M., Gerwien, J., Nissen, M. H., Thøgersen, H. C., and Buus, S. (1995) *Eur. J. Immunol.* **25,** 1609–1616
21. Shields, M. J., Moffat, L. E., and Ribaudo, R. K. (1998) *Mol. Immunol.* **35,** 919–928
22. Achour, A., Michaëlsson, J., Harris, R. A., Ljunggren, H. G., Kärre, K., Schneider, G., and Sandalova, T. (2006) *J. Mol. Biol.* **356,** 382–396
23. Bertoletti, A., Chisari, F. V., Penna, A., Guilhot, S., Galati, L., Missale, G., Fowler, P., Schlicht, H. J., Vitiello, A., and Chesnut, R. C. (1993) *J. Virol.* **67,** 2376–2380
24. Bertoletti, A., Sette, A., Chisari, F. V., Penna, A., Levrero, M., De Carli, M., Fiaccadori, F., and Ferrari, C. (1994) *Nature* **369,** 407–410
25. Bertoletti, A., Southwood, S., Chesnut, R., Sette, A., Falco, M., Ferrara, G. B., Penna, A., Boni, C., Fiaccadori, F., and Ferrari, C. (1997) *Hepatology* **26,** 1027–1034
26. Krutzik, P. O., and Nolan, G. P. (2006) *Nat. Methods* **3,** 361–368
27. Hadrup, S. R., Bakker, A. H., Shu, C. J., Andersen, R. S., van Veluw, J., Hombrink, P., Castermans, E., Thor Straten, P., Blank, C., Haanen, J. B., Heemskerk, M. H., and Schumacher, T. N. (2009) *Nat. Methods* **6,** 520–526
28. Newell, E. W., Klein, L. O., Yu, W., and Davis, M. M. (2009) *Nat. Methods* **6,** 497–499
29. Kessler, J. H., Mommaas, B., Mutis, T., Huijbers, I., Vissers, D., Benckhuijsen, W. E., Schreuder, G. M., Offringa, R., Goulmy, E., Melief, C. J., van der Burg, S. H., and Drijfhout, J. W. (2003) *Hum. Immunol.* **64,** 245–255
30. van der Burg, S. H., Ras, E., Drijfhout, J. W., Benckhuijsen, W. E., Bremers, A. J., Melief, C. J., and Kast, W. M. (1995) *Hum. Immunol.* **44,** 189–198
31. Glithero, A., Tormo, J., Doering, K., Kojima, M., Jones, E. Y., and Elliott, T. (2006) *J. Biol. Chem.* **281,** 12699–12704
32. Rodenko, B., Toebes, M., Celie, P. H., Perrakis, A., Schumacher, T. N., and Ovaa, H. (2009) *J. Am. Chem. Soc.* **131,** 12305–12313